DEVELOPMENT OF A PORTABLE GRAPHITE CALORIMETER FOR PHOTONS AND ELECTRONS

M R MCEWEN, S DUANE
Centre for Ionising Radiation Metrology,
National Physical Laboratory,
Teddington, Middlesex, UK
TW11 0LW

Abstract

The aim of this project is to develop a calorimeter for use in both electron and photon beams. The calorimeter should be more robust than the present NPL primary standard X-ray calorimeter and is designed to be sufficiently portable to enable measurements at clinical accelerators away from NPL. Although intended for therapy-level dosimetry, the new calorimeter can also be used for high-dose measurements at industrial facilities. The system consists of a front end (the calorimeter itself), means for thermal isolation and temperature control, and a measurement system based on thermistors in a DC Wheatstone bridge. The early part of the project focussed on the development of a temperature control system sensitive enough to allow measurements of temperature rises of the order of 1 mK. The control system responds to the calorimeter, phantom and air temperatures and maintains the temperature of the calorimeter to within ± 0.2mK over several hours. Initial operation at NPL in X-ray and electron beams show that the system is capable of measurements of 1 Gy at 2 Gy/min with a random uncertainty of ± 0.5% (1 standard deviation). The result of comparing the calorimeter with the present primary standard calorimeter in 6, 10 and 16 MV photon beams is very encouraging, giving agreement within 0.5% at all energies measured, which is within the measurement uncertainties. The results in a 16 MeV electron beam are somewhat confusing, showing a discrepancy of approximately 5%. There is no obvious reason for this discrepancy, although a possible cause is charge storage in the calorimeter core due to poor earthing. Further work is required to investigate this problem, as well as carry out a wider range of measurements in both photon and electron beams.

ISSN 1369-6793

National Physical Laboratory
Teddington, Middlesex, United Kingdom, TW11 0LW

Approved on behalf of Managing Director, NPL,
by J B Hunt, Head of Centre, Centre for Ionising Radiation Metrology

CONTENTS

TABLES

FIGURES

1. INTRODUCTION

Graphite calorimeters have been under development at NPL for many years. There are separate primary standard graphite calorimeters for high energy photon and electron beams. The photon calorimeter (DuSautoy, 1996) is based on the design by Domen and Lamperti (1974) and is a complex device able to measure doserates down to 1 Gy/min. The electron beam calorimeter was first developed for high dose applications in radiation processing and sterilization (Burns *et al*, 1994) but has been enhanced to operate at radiotherapy doserates as low as 5 Gy/min (McEwen *et al*, 1998). Graphite has obvious advantages as the material to use for a calorimeter in that it is a solid with a high thermal conductivity and zero heat defect (i.e. all the energy deposited by the radiation is expressed as heat). However, its major limitation is that it is not the material of interest. In the majority of dosimetry applications absorbed dose to water is the quantity required and, therefore, corrections are required to convert from absorbed dose to graphite to absorbed dose to water. A water calorimeter would give the desired quantity directly, but water calorimeters tend to be very complex devices and the radiochemical reactions in water lead to a heat defect which makes it difficult to obtain an accurate value of the absorbed dose. Water calorimeters are under development at a number of institutions worldwide - including NPL - and their use is generally restricted to radiotherapy dose levels.

Since the two graphite calorimeters at NPL are of very different designs, it is not possible to define either one as the primary standard for both radiation types. The photon calorimeter can operate in high energy photons from ^{60}Co to 20 MV but is restricted to electron energies above 12 MeV. The electron calorimeter's simplicity of design means that it cannot operate at the limited doserates available for high energy photons. It would be preferable to have a single calorimeter for both electron and photon beams for a range of doserates - from therapy levels up to industrial levels.

NPL offers a number of dosemeter calibration services for high energy photon and electron beams at therapy and industrial doserates. One area of concern for all these services is the validity of the transfer of the calibration from NPL to other radiation facilities. It is assumed that the secondary dosemeters calibrated, whether they are ion chambers or chemical dosimeters, behave in the same way in two radiation beams defined by some beam quality. It is difficult to test this assumption since it has not been generally possible to operate primary standard calorimeters away from NPL. It is a desirable objective to be able to operate a calorimeter in the user's own radiation field. This would enable one to check the transfer of calibrations and investigate beam quality issues. This is primarily a concern at radiotherapy dose levels where the uncertainty associated with a calibration has to be much smaller, but it would also be beneficial to have a calorimeter that could be taken to industrial facilities.

2. DESIGN

2.1. Design requirements

The design requirements of this new calorimeter can be stated quite simply:

(1) A single calorimeter to operate in high energy photon beams (Co-60 gamma rays and 4 MV to 20 MV X-rays) and electron beams (3 MeV to 25 MeV) at doserates from 1 Gy/min to 10 kGy/min.

(2) A simple and robust design, easy to maintain.

(3) Portable, to allow measurements at other radiation facilities, primarily in the UK but also in other countries.

There are two main problems with therapy-level calorimetry - measuring the radiation-induced temperature rise, and preventing environmental changes from swamping the measurement. The radiation-induced temperature rise in a material is related to the absorbed dose via the specific heat; a dose of 1 Gy (a typical dose at radiotherapy levels) to graphite leads to a temperature rise of 1.4 mK. To be useful, the calorimeter must be able to measure this dose with an uncertainty better than ± 0.5%, which is equivalent to ± 7μK. To resolve temperatures to this level at room temperature is a severe problem requiring state-of-the art equipment. The second problem is that of temperature control. To be able to measure the radiation-induced temperature rise in the calorimeter, environmental effects must be kept to a minimum. The radiation-induced temperature rise is obtained by extrapolating the pre- and post-irradiation temperature traces to the mid-point of the irradiation. Changes in these traces due to environmental effects would result in an error in the extrapolation. Ideally, the pre- and post-heat temperatures should be constant, but a linear drift in one direction does not have an effect on the extrapolation. However, any non-linear behaviour in the drift would significantly affect the derivation of absorbed dose. This, therefore, implies that the room where the calorimeter is used must have very stable air conditioning, or the calorimeter must have built-in temperature control. The NPL linear accelerator (LINAC) benefits from a very stable air-conditioning system which keeps the temperature of the irradiation room at ± 0.1 °C, allowing operation of the electron beam calorimeter down to 5 Gy/min with only minimal expanded polystyrene insulation. However, such air conditioning is not generally available in other radiation facilities and therefore the only option is to design a calorimeter with built-in temperature control. Such a control system would have to cope with a wide range of temperatures and rapid temperature changes. For example, a LINAC exposure room in a radiotherapy clinic has a maze entry but no doors, and therefore a calorimeter in such a room could experience a combination of effects due to draughts and heat sources (e.g. the LINAC itself). The situation in industrial facilities is likely to be even more severe, although the measured temperature rise due to the radiation is much larger.

2.2. Calorimeter design

After some consideration it was decided to base the new calorimeter on the present electron beam primary standard calorimeter. Such a device would need further enhancements to allow operation at 1 Gy/min and in more hostile environments than those found at NPL. Graphite was the material of choice since there was already much experience of using graphite calorimeters at NPL. The only other choices are water or water-equivalent plastic. Water is not practicable for a portable calorimeter and little work has been done on plastics, except for polystyrene. Although the conversion from graphite to water adds an additional uncertainty, it was not felt to be a significant problem. The basic elements of the calorimeter are shown schematically in Figure 1. The main calorimeter body is a graphite core and a graphite surround. The core is a disc 20 mm in diameter and 2 mm thick, with holes drilled radially into the disc to accommodate four 22 kΩ bead thermistors of diameter 0.5 mm and length 3 mm. The graphite surround is an octagon 90 x 90 mm in cross section and 6 mm in thickness. The core is thermally isolated from the surround by a nominal 1 mm air gap at all faces and is supported by small expanded polystyrene beads. The octagon is a convenient approximation to the nominal 90 mm diameter circular field of the NPL LINAC at a SSD of 1 m. The thickness of the calorimeter core is chosen so that it can be used in the lowest electron energy available from the NPL LINAC - 3 MeV. The diameter of the core is such that any correction for radial beam uniformity is small.

Graphite plates are added in front of the calorimeter body to position the core at the desired measurement depth and also added to the rear to provide backscatter. The optimal thickness of this backing depends on the radiation type, the incident beam energy and on the measurement depth and is chosen so that the temperature rise in the backing is as close as possible to that in the core. One of the major problems with electron dosimetry is the rapid fall-off of the depth-dose curve. If one used a traditional "thick" phantom, such as employed in the photon primary standard calorimeter, there would be significant heat transfer from the core to the graphite surround (especially without the benefit of a vacuum system) making extrapolations more uncertain. The entire calorimeter assembly is enclosed in 25 mm of expanded polystyrene to provide a first level of thermal isolation.

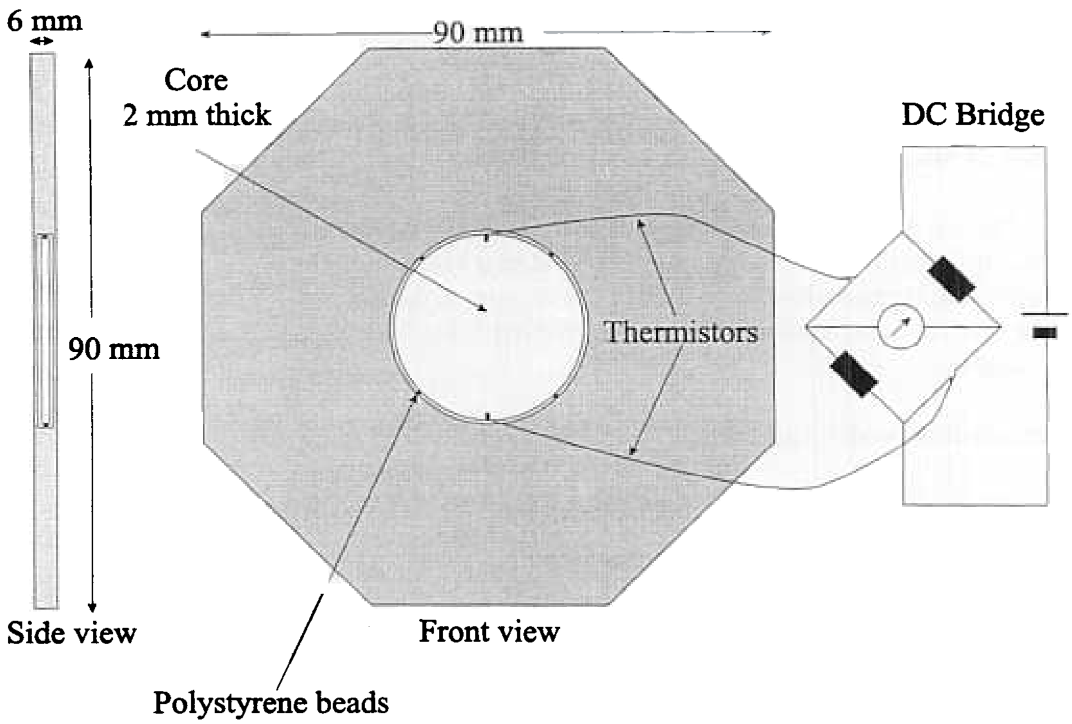

FIG. 1. *Schematic diagram of calorimeter. For clarity the second bridge and associated thermistors are omitted.*

The thermistors that measure the temperature rise in the graphite core are included in opposing arms of two simple DC Wheatstone bridges constructed from precision resistors with a very low temperature coefficient (<1 ppm/°C). Two commercial 6½-digit voltmeters (DVMs) read the out-of-balance voltages from the bridges simultaneously and are operated under IEEE-488 computer control. The power supply for the bridge is a precision voltage supply (V_{sup} equivalent to 1.4 V) constructed at NPL (Sanders and Thomas, 1991). The aim of these enhancements to the basic electron calorimeter design was to increase the signal to noise ratio. Two bridges give an immediate improvement. By using thermistors in opposing arms of the bridge one can cancel out some of the induced noise, which theory suggests should be better than single thermistors in individual bridges. Shielded, twisted-pair cable is used throughout to keep noise pickup to a minimum - a linear accelerator is a very electrically noisy environment and therefore every precaution must be taken to minimise the effects of noise. A larger value of the bridge supply can also be used to increase the signal-to-noise ratio, although it also increases the power dissipated in the thermistors and raises the question of non-linear effects due to thermistor self-heating. Calculations have indicated that a value of up to 2 V can be used safely.

The bridge out-of-balance voltage is calibrated directly against the absolute core temperature using a commercial platinum resistance thermometer (PRT). The thermistors used in the calorimeter have been found to be very stable requiring re-calibration only every two years. The effect of accumulated dose on the response of the thermistor type used here has been measured at NPL (McEwen et *al*, 1993). No change was measured at the ±0.1% level for doses in excess of 1 MGy.

As stated earlier, the absorbed dose to the graphite core D_g is derived directly from the absolute temperature rise ΔT_g and specific heat capacity c_g of the core ($D_g = c_g \times \Delta T_g$). Extensive measurements have been carried out at NPL to measure the specific heat capacity of the graphite core over the temperature range 18-32 °C. Williams (1993) looked at several samples of graphite and found no significant difference in the specific heat capacity. He also irradiated a sample up to a dose of 3 MGy and re-measured the specific heat capacity. Again, there was no significant difference in the result. The result also agreed with previous measurements of the specific heat capacity made at NPL using the method of differential scanning calorimetry (Richardson, 1984), but with a much reduced uncertainty.

The most significant drawback of this design is the limited isolation of the core from the surround. By using only a 1 mm air gap, rather than a vacuum gap as in the photon primary standard calorimeter, one increases the heat transfer from the core to the surround. If the time constant associated with this transfer is too small then what is measured is the bulk temperature rise rather than the core temperature rise.

2.3. Temperature control system

The temperature control system is shown schematically in Figures 2 and 3. It consists of a large graphite body (total mass 14 kg) which surrounds the calorimeter on five sides. It is not possible to put material in front of the calorimeter since that would affect the measurement depth and prevent operation at the lowest electron energies. Embedded within the graphite body are electrical heater elements which elevate the body temperature to approximately 30 °C. By operating at an elevated temperature one can use the environment as the cooling circuit rather than employing Peltier heat engines. The entire body is surrounded by 25 mm of expanded polystyrene, with an extra 50 mm at the front to reduce the heat transfer from the environment to the calorimeter. This polystyrene is enclosed in a hard plastic case, open at the front, which is electrically screened to reduce noise pickup. The current to the heater elements is provided by a computer-controlled power supply. Three temperatures are sensed - the calorimeter surround, graphite body, and outside air. An algorithm running on the controlling PC adjusts the heater current according to the temperatures of the air, body and calorimeter surround in order to keep the calorimeter temperature constant, at 29 °C. An alternative to this system would be to place the calorimeter inside an air-conditioned box. However, to obtain the same stability as the graphite body arrangement one would need such a large volume of air that the system would no longer be portable. The overall dimensions of the body controller are 40 x 40 x 40 cm which makes it relatively easy to transport. It should be noted that there are no heater elements in the calorimeter itself and that the body is outside the NPL LINAC beam (except behind the calorimeter). This design is therefore best suited to a scattered, rather than swept, beam.

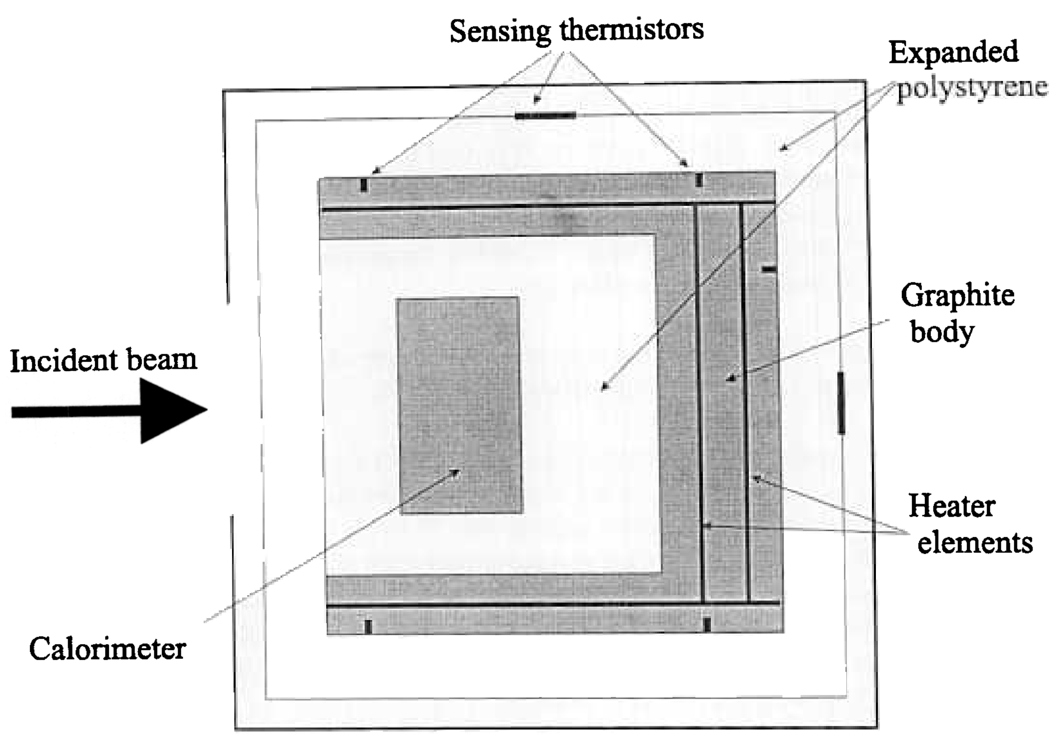

FIG. 2. Schematic diagram of the body design - side view.

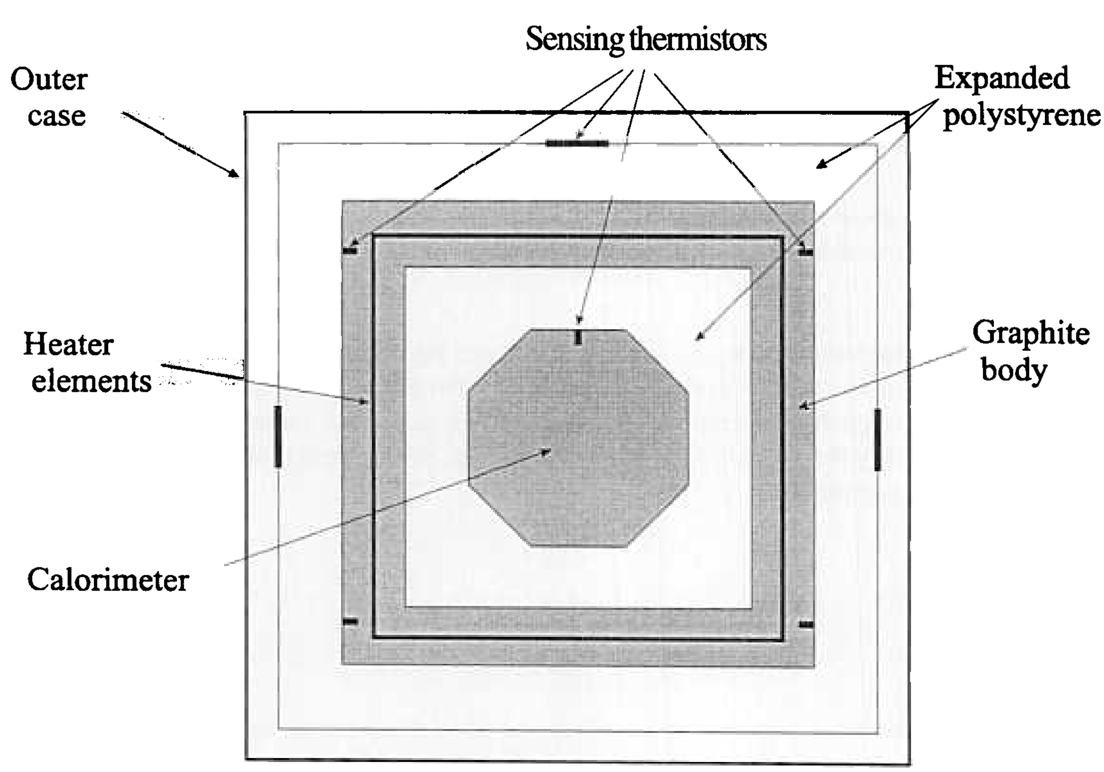

FIG. 3. Schematic diagram of the body design - front view.

The temperature sensing thermistors used for the control system are separate from those used to determine the absorbed dose. The sensor for the calorimeter surround is a single glass bead thermistor in a DC bridge. The graphite body uses nine thermistors in a series/parallel arrangement in a single arm of a DC bridge. This arrangement behaves like a single thermistor but gives the mean temperature over the whole of the graphite body. Similarly, the air is sensed using four thermistors in a series/parallel arrangement to give the mean air temperature over four sides of the outer case. These air sensors are mounted on thin graphite plates to reduce any self-heating effect and give a more reliable response. The three temperature sensors are calibrated in terms of absolute temperature against a PRT in the same way as the thermistors used to measure the absorbed dose.

Separate PCs are used to control the calorimeter temperature and measure the absorbed dose - although this involves more equipment it simplifies the software.

The calorimeter tends towards thermal equilibrium with its environment. Making simple but reasonable assumptions, a model can be set up in which this environment is equivalent to a suitably weighted average of the sensed air and body temperatures. The control algorithm adjusts the power to the body heater so as to maintain this weighted average temperature at a constant value, normally 29 °C. To the extent that the model is valid, it should be that the calorimeter relaxes towards this constant temperature and, provided the air is always cooler than the calorimeter, the effect on the calorimeter of variations in air temperature should be cancelled by variations in the body temperature. (This control algorithm is referred to below as quasi-core constant.)

It turns out that the time constant for 'settling' of the calorimeter temperature is about 6 hours, which is rather too long for equilibrium to be achieved overnight, as would be required for measurements in the field. The approach to equilibrium can be accelerated by overheating the body when the calorimeter is cool and warming too slowly, and reducing the power to the body heater when the calorimeter is cool but warming too quickly (or warm but cooling too slowly). The same model as above can be used to make this qualitative idea quantitative, and the result is a control algorithm (referred to below as core constant) for which the time constant is reduced to 1 hour. In this version, variations in the calorimeter temperature have a direct effect on the body electrical heating power, which in turn affect the rate at which the calorimeter temperature drifts. This is to be avoided during radiation measurements, when the pre- and post-heating drifts in the core temperature are extrapolated to determine the absorbed dose.

In the NPL LINAC exposure room, the room temperature control is sufficiently close that, once the system has reached equilibrium, it is enough to maintain the body temperature constant, ignoring the (essentially constant) sensed air temperature. This control algorithm (referred to as body constant) eliminates the possibility that variations in electrical heating power might introduce a systematic error into the radiation measurements.

3. TESTING

3.1 Electrical noise

As mentioned above, minimising the electrical noise is a priority, and therefore the first stage of testing the calorimeter. A number of the polyimide thermistor probes were constructed, tested and the ones exhibiting the lowest noise were used in the calorimeter core. Two dual-bridge units with slight constructional differences (different types of enclosure and connectors, different methods of fixing the resistors in position) were used to investigate how construction might affect the inherent noise of the bridge. As for the thermistors, the unit with the lowest noise was used for the radiation testing. A comparison was also made between twisted-pair and co-axial cable. The effect of shielding the outer case was also investigated and the opportunity was taken to compare the performance of various types of DVM. The required uncertainty of ± 7 μK is close to the resolution of a 6½-digit voltmeter and therefore a 7½-digit instrument could give improved resolution and, possibly, precision. However, DVM resolution has to be considered against acquisition time since both have a direct effect on the extrapolations to determine the absorbed dose.

3.2 Temperature control

Significant effort has been put into developing the control algorithm, outlined above. The control system is somewhat asymmetric in that the body temperature rises much more rapidly at maximum heating power than it falls at zero power. Symmetry could be restored by selecting a higher operating temperature, at the likely cost of greater sensitivity to room temperature variations. The system has been tested in a variety of environments and in various modes of operation, in order to determine the heat transfer coefficients for the three components - air:body, air:calorimeter and body:calorimeter. These depend on the heat capacity of the calorimeter, and so the behaviour of the system varies according to the amount of graphite build-up and backing plates. The likely performance in other, less stable environments than NPL has been evaluated by subjecting the system to periodic variations in room temperature.

3.3 Calorimeter performance

The next step was to investigate the performance of the calorimeter, including any systematic effects, and validate it against the present primary standards at NPL. The calorimeter was tested in 6, 10 and 16 MV photons and 16 MeV electrons using the NPL linear accelerator. The NPL LINAC is a travelling-wave, two-section research accelerator allowing manual control of all the important operating parameters (pulse current, prf, pulse width, *etc*) at any electron energy in the range 3-20 MeV. A tungsten target (for X-rays) or an aluminium scatter plate (for electrons) is placed at the end of the accelerator flight tube. For the photon measurements a SSD (source-surface distance) of 1 m and field size of 9 cm diameter was used; for the electron measurements a SSD of 2 m and a field size of 15 cm × 15 cm was used. The doserate for photons was varied between 2 and 5 Gy/min while in electrons a higher doserate between 10 and 20 Gy/min was used. By operating at higher doserates one can give the required dose (typically 1 Gy) in a much shorter time and therefore one can investigate more thoroughly the transfer of heat between the calorimeter core and its immediate surround. It is obviously easier to obtain the higher doserates in electrons. A transmission monitor ion chamber is used to correct for current variations in the LINAC output. This monitor is of an NPL design - aluminium electrodes are evaporated onto 25 μm polyimide foils - putting a minimal amount of material in the beam. LINAC pulse repetition frequencies of 200 Hz and 240 Hz were used and the length of the calorimeter irradiations was determined by the number of pulses delivered by the LINAC.

Rather than use the photon primary standard, the calorimeter was compared in X-rays with a calibrated NE2611 ionisation chamber. NPL maintains a number of these chambers, which are used to calibrate other user chambers and are calibrated themselves against the primary standard on a yearly basis. In the electron beam the calorimeter was compared both with the electron beam calorimeter and a calibrated NACP ionisation chamber. The phantom used in this new calorimeter is much smaller than those previously used. There is a difference in the dose contribution from scattered radiation for which a correction is required before comparing the results from both systems. This effect is likely to be larger for the electron beam where the field size is much larger than the calorimeter phantom. There is also the effect of the body to be taken into account. Although the body is not directly in the beam, there will also be a scatter contribution to the dose measured by the calorimeter core. Measurements were therefore carried out to determine the size of this scatter correction in 10 and 16 MV photons and 16 MeV electrons.

4. DISCUSSION OF RESULTS

4.1 Electrical noise

Qualitative and quantitative measures were used in assessing noise rejection. Calorimeter runs were viewed graphically and visual comparisons made. The data was then fitted with a linear fit and the RMS deviation used as a measure of the noise in the signal, expressed in terms of temperature. These results are summarised in Table 1.

Table 1 Results of noise testing

Component under test	Type/identifier	RMS deviation (μK)	RMS deviation (μK) normalised
Bridge	A	9.1	10.0
Bridge	B	9.5	10.4
Cable	Twisted pair cable	9.4	10.0
Cable	Co-axial cable	10.4	11.1
DVM	7061	8.6	10.0
DVM	2182	10.2	11.9
DVM	1271	13.3	15.5
Calorimeter	Unshielded	11.7	10.0
Calorimeter	Shielded	7.3	6.2
Calorimeter	Electron calorimeter	10.9	9.3

Initial testing of the thermistors indicated that the connectors were critical to minimising the noise. After some investigation it was found that LEMO 00 series (two-pole) gave the best combination of reliability and low noise. Six thermistor assemblies were tested and two were obviously more noisy than the others and were therefore rejected.

There was very little difference in the performance of the two bridge units. The source of electrical noise is often difficult to identify and solder joints/connections are obvious possibilities. The fact that the two bridges showed similar performance indicates that either the joints are good, or they are equally bad in both bridges. There was no difference between the two bridges in each unit. Further refinement of the bridge design is possible by the use of PCB techniques to provide more reliable joints and a larger ground plane.

The difference in the performance of the twisted-pair and co-axial cables was smaller than expected, with the twisted-pair giving approximately 10% less noise (equivalent to 1 μK). Twisted-pair cable gives more noise immunity from magnetic fields, while co-axial cable is better for electric fields. It is generally thought that for a DC bridge in the environment of the linear accelerator, twisted-pair cable gives the lowest noise, but this has not been proved here.

A number of DVMs were tested - Solartron 7061, Wavetek 1271, Keithley 2001 and Keithley 2182. The 7061 is the standard DVM used, combining 6½-digit resolution with a reasonably fast acquisition time (0.2 s) and good noise rejection. The other three DVM types were all found to suffer from the same problem - although they have 7½-digit capability, the acquisition time for that resolution was either too long (of the order of 2 s) or the noise rejection wasn't as good as obtained with the 7061. The Wavetek 1271 DVM was the best of rest, offering a faster acquisition time at 6½-digits (0.1 s) but at the price of a noisier signal. The possibility of shielding the DVMs was also investigated but no improvement was observed.

The largest improvement in noise reduction was through the use of electrical shielding around the calorimeter outer case, as shown in Table 1. Without the shielding in place, the calorimeter signal shows large excursions which would make the extrapolations very inaccurate. High frequency noise is not a big problem for calorimetry since the fitting routines used in the extrapolations are very effective. The shielding is very effective in removing the low frequency noise (<0.2 Hz) and reducing the RMS deviation by approximately a factor of 1.6. By way of a comparison, the noise of the electron calorimeter was also measured and found to be as good as the unshielded calorimeter. This is somewhat surprising since the electron calorimeter does not benefit from the cancellation effect of two thermistors in the bridge. However, the electron calorimeter has shorter cabling which will reduce the amount of pickup and may explain the lower noise. The combination of the reduced noise in the new calorimeter and the two bridges gives an improvement in the signal-to-noise over the electron calorimeter of greater than two. This, along with the very stable temperature control, should allow operation of the calorimeter down to doserates of the order of 1 Gy/min.

4.2 Temperature control

Figure 4 shows the variation in the temperature measured by the various temperature sensors when the control program is started. Initially the calorimeter is at room temperature with all three sensors reading the same temperature. As stated earlier, rapid stabilization of the calorimeter at its operating temperature is a primary requirement of the algorithm, and this is achieved by rapidly heating the body above its operating temperature and then, at the appropriate moment, switching the electrical heating off. This makes the calorimeter temperature drift up to the desired operating temperature and, just before its temperature would start to fall again, the body is turned on again to maintain constant temperatures. The user is able to set the required temperature of the calorimeter and the control program adjusts the body temperature to suit, depending on the air temperature. As can be seen the air sensor also indicates an increase in temperature. This is because the air sensors are placed on the outside of the case of the body and respond to heat conducting through the polystyrene insulation. Although this means that the air sensors do not measure the true air temperature, it does not significantly affect the performance of the control program. Stabilization of the calorimeter is achieved within eight hours.

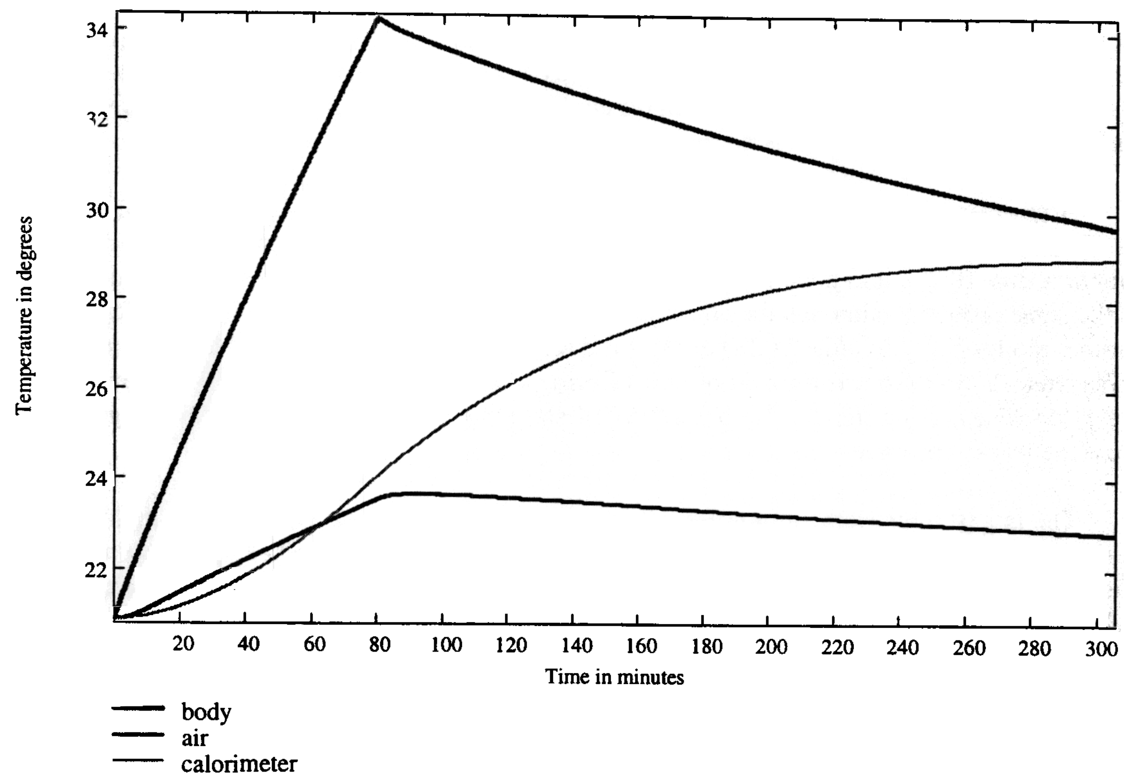

FIG. 4. Performance of temperature control system from switch on

Figure 5 shows the stability of the calorimeter at a later time when stabilization has been achieved. By varying the body temperature in response to air temperature variations, the calorimeter temperature is maintained to ± 0.2 mK over several hours. As one can see, there is a slight systematic residual in the calorimeter temperature (at the 0.1 m K level) indicating that the control algorithm isn't fully correcting for air temperature variations. Although the long term stability is impressive, one is really interested in the stability of the system over the length of a calorimeter run - typically five minutes. Slow changes in temperature are acceptable since these produce linear drifts in the calorimeter trace and these are typical of the NPL environment. It is not so certain that other radiation facilities are so benign. One of the concerns in developing the algorithm was whether the parameters determined in the model were 'universal' or situation specific. Ideally the control program would perform in the same manner in any radiation facility, but further work is required to see whether this is true. Work is currently underway at NPL to gain a deeper understanding of the physical processes involved in the calorimeter system which should yield a more robust and reliable control algorithm.

As stated above, the program has a number of control modes and the three commonly used are:

(1) Body constant - no attempt is made to control the calorimeter temperature.
(2) Core constant - the body is varied to keep the calorimeter at a fixed temperature.
(3) Quasi-core constant - the body is varied in response to changes in the air temperature but no account is taken of the actual calorimeter temperature.

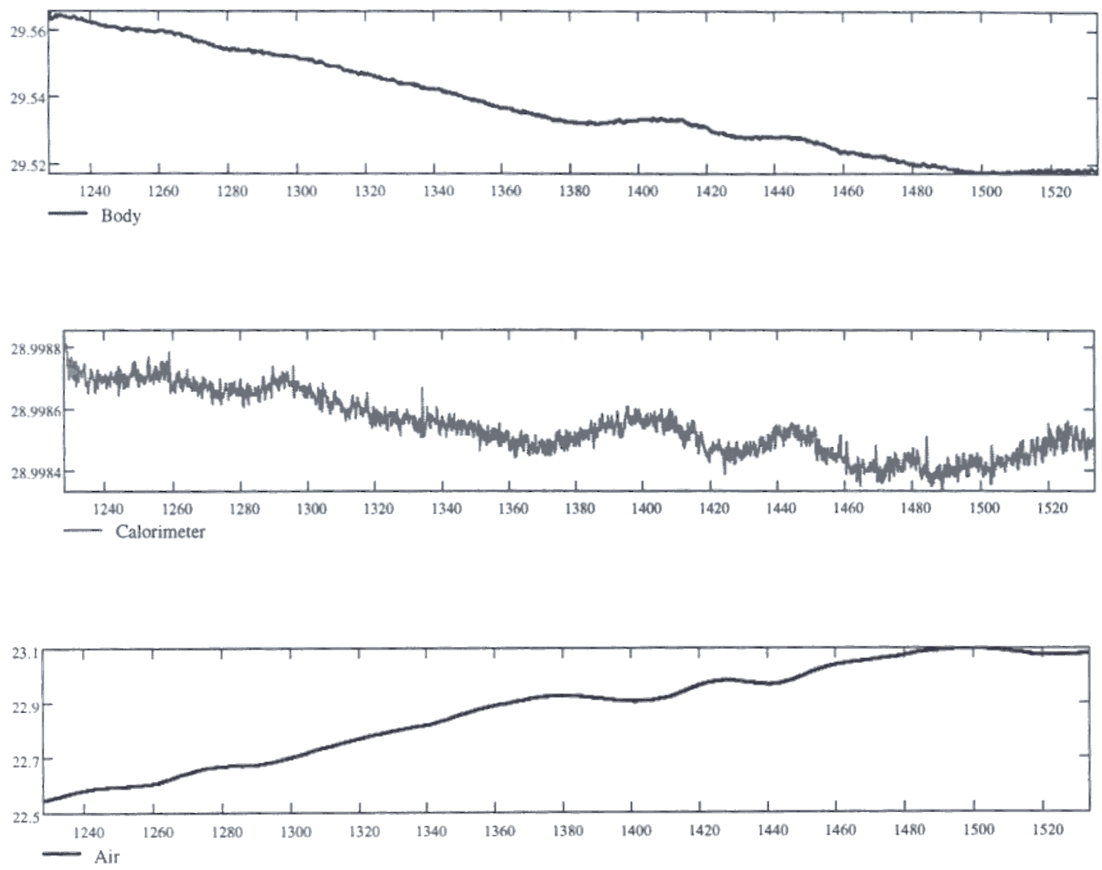

FIG. 5. Stability of temperature control system. X axes - time (min), Y axes - temp (°C)

The normal mode used for calorimetry is Mode (1), although Mode (3) was also used during the radiation tests. Figure 6 shows the response of the control program during a calorimeter run when operated in Mode (2). The program sees the radiation induced temperature rise in the calorimeter and adjusts the body temperature to counteract the effect. This affects the heat transfer from calorimeter to body and changes the shape of the post-irradiation calorimeter trace. The calorimeter signal in Figure 6 also shows a level of noise greater than one would expect for the DC bridge system used. The most likely explanation is a fault in the thermistor connections. In Mode (2), the calorimeter signal directly affects the body temperature set by the control program, and a high level of noise in the sensing thermistor will result in fluctuations in the control temperature.

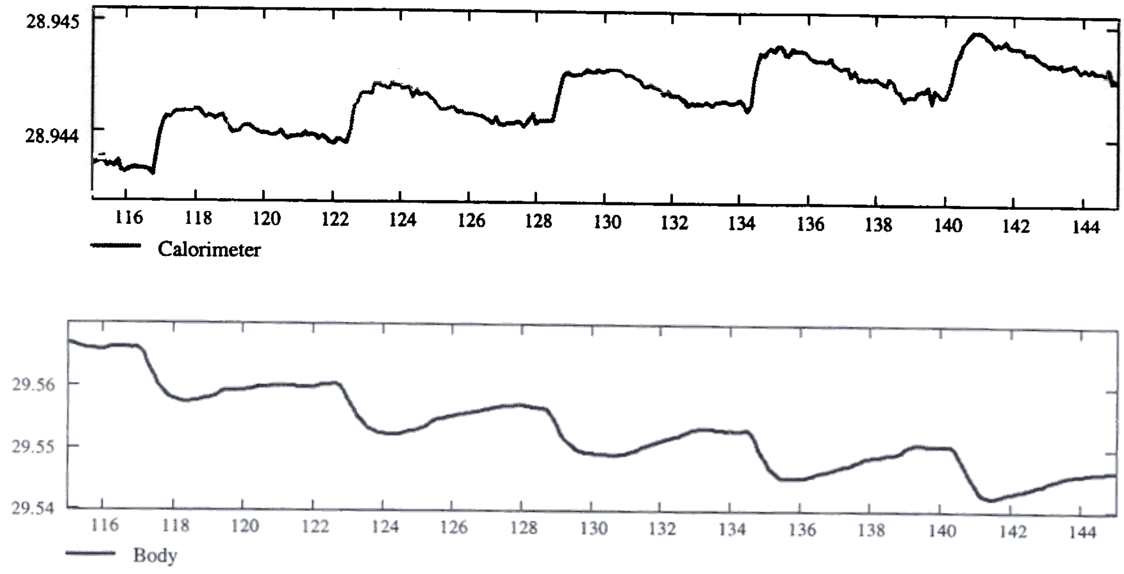

FIG. 6. Response of body to changes in calorimeter temperature in core-constant control mode X axes - time (min), Y axes - temp (°C)

4.3 Calorimetry

4.3.1 Calorimeter performance

A primary requirement in carrying out calorimetry is stability of the LINAC output. Beam current variations are taken into account by use of the transmission monitor, but a change in mean energy will change the calorimeter or ion chamber reading per monitor unit. Stability is not crucial if one is just looking at the performance of the calorimeter alone, but is necessary when comparing with the primary standards. The two devices being compared are alternated in the beam on a regular basis to minimise the effects of LINAC drift, but this cannot correct for a step change in energy. Normally, the NPL LINAC is very stable, generating a narrow electron spectrum. However, the ion chamber measurements made during each day showed a larger spread than one would expect, indicating that the LINAC output energy was changing. If one could measure the generated electron spectrum for each measurement then one could correct for these changes but this is not really an option since it would significantly reduce the amount of useful beamtime available during the day. However, the LINAC output was stable enough to produce useful results.

Figure 7 shows a typical calorimeter run in a 16 MV photon beam at a doserate of 5 Gy/min. The irradiation time was kept to a minimum so that any heat transfer between core and surround in the calorimeter would be clearly seen. If one had complete isolation of the core from the surround then the post-heat trace would have exactly the same gradient as the pre-heat trace, but this is obviously not the case here. Curvature in the post-heat trace indicates significant heat transfer from core to surround. The extrapolations will correct for this heat loss but the measurement uncertainty is increased due to the non-linear behaviour. This effect can be minimised by using short irradiation times but one is constrained by the signal-to-noise ratio which, at present, limits the minimum measurable dose to about 0.5 Gy. The typical standard deviation in the calorimeter/monitor ratio for ten calorimeter runs is ± 0.5%. This is the random uncertainty and is due to a combination of effects including noise, extrapolations and drifts in

LINAC output, and is slightly larger than one would like. It is hoped to further improve the signal-to-noise, which should reduce this uncertainty.

A problem that became apparent during the testing of this calorimeter was the reliability of the transmission monitor. Initial testing in photons used a PTW-design monitor (Type 7862). A chamber of same type had been tested previously and found to behave well. However, this chamber showed a strange settling effect in that it required several minutes of beam to give an equilibrium reading. This monitor was replaced by a NPL-design chamber. Although McEwen [4] had noted a problem with an earlier chamber of this design, this chamber behaved well throughout testing.

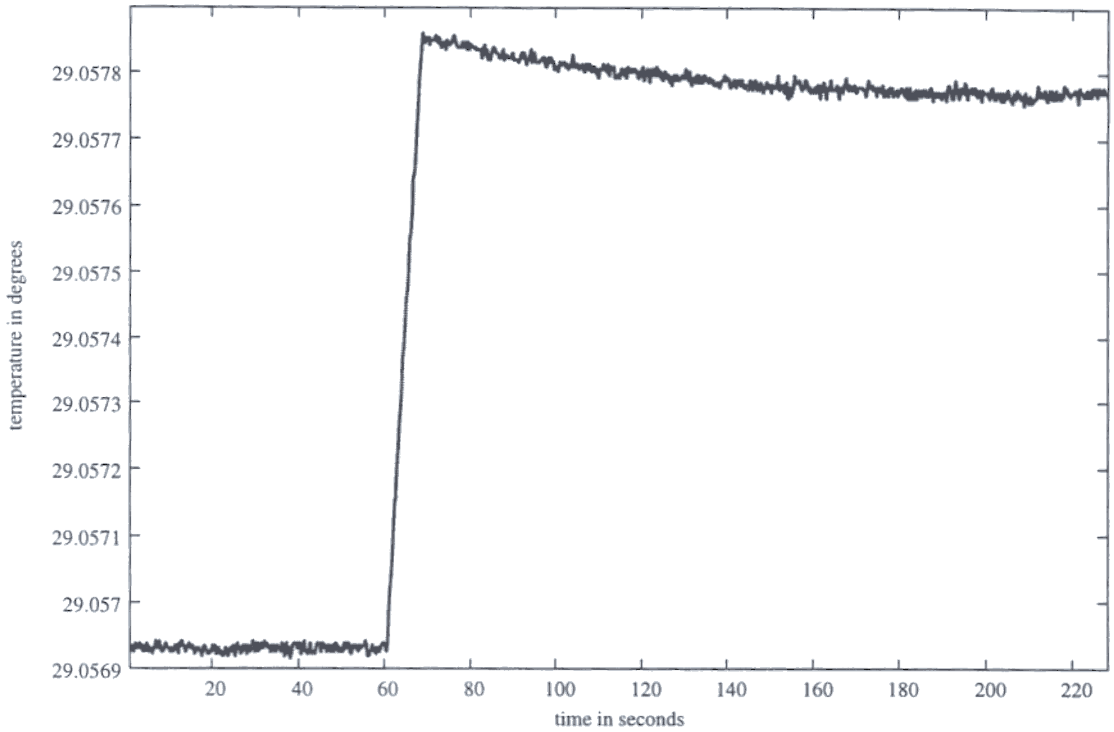

FIG. 7. Typical calorimeter run at NPL in a 16 MV photon beam at a doserate of ~ 5 Gy/min

4.3.2 Corrections

There are various corrections required in the derivation of absorbed dose. Ion chamber measurements need to be corrected for the effect of ion recombination. Plots of the reciprocal of the current against the reciprocal of the voltage were made at a number of doses per pulse to determine the recombination correction according to the standard Boag (1950) theory. It was found that the correction is only dependant on dose-per-pulse and chamber HT and not electron energy (Burns and McEwen, 1998). The correction is then defined in terms of the charge per pulse collected by the chamber, Q_{coll}, at a fixed polarising voltage as follows:

$$p_{ion} = c + mQ_{coll} \tag{1}$$

The constants c and m are derived from measurements at a number of doserates and the coefficients for the NPL reference chambers are given in the Table 2. These coefficients allow on-line correction rather than performing recombination measurements each time the chamber is used. The uncertainty in the recombination correction is estimated to be ± 0.1% at the 95% confidence level.

Table 2 Recombination coefficients for NPL reference chambers

Chamber type	Serial no.	c	m (pC^{-1})	HT (V)
NE2611	122	1.0014	0.002300	200
NACP-02	30-09	1.0021	0.002659	100
NACP-02	37-01	1.0005	0.003278	100

Although the build-up thicknesses for calorimeter and chamber are matched, the finite sizes of graphite plates available mean that corrections are required for slight differences in measurement depth. Corrections were obtained from depth-ionisation measurements. Included in this correction factor is the averaging effect of the 2 mm thick calorimeter absorber, compared to the chamber measuring at a point (taken as the centre of the chamber for the NE2611 and the inside the front face for the NACP). A further correction is required to account for a difference in the SSD of the calorimeter or chamber.

As mentioned above, there is a difference in scatter between the devices being compared. Firstly, there is the scatter effect due to the calorimeter body, which is required for both photons and electrons. Secondly, there is correction in electron beams to convert from the small (9 cm x 9 cm) phantom used here to the larger (15 cm x 15 cm) phantom used in the electron calorimeter.

A correction is required for beam uniformity - the diameter of the calorimeter core is 20 mm, the diameter of the electron calorimeter core is 50 mm, the diameter of a NE2611 chamber is approximately 8 mm, while that of the NACP chamber collecting volume is 10 mm. The experimental geometry is chosen to minimise the effects of beam non-uniformity, although a correction is still required, which is obtained from beam scans. In photon beams, beam scans were obtained using a PTW LA48 linear ion chamber array. This is an array of 47 liquid-filled ion chambers which gives an instantaneous readout of the beam uniformity. However, this only operates up to 5 Gy/min; therefore beam scans in electron beams were obtained by moving the NACP chamber across the beam in the graphite phantom at the relevant measurement depth. Typical beam scans at a number of photon energies are shown in Figure 8. As can be seen, the field size and beam flatness are the same at all energies. The only difference is the in the penumbra, which increases with energy as would be expected.

A correction is also required for the 1 mm air gap around the calorimeter core. Initial results for the X-ray qualities yield a value of approximately 0.7%. Cottens *et al* (1981) carried out a series of measurements looking at the effect of the vacuum gaps in a Domen-type calorimeter (similar to the NPL photon primary standard) and saw a maximum effect of 0.7%, which is in good agreement with these calculations. The gap effect for electron beams has not yet been determined but measurements in electron beams with air gaps of 0.5 mm and 1 mm have indicated that the correction is less than 0.3%. It is assumed that this calorimeter has a similar gap effect, although this is smaller than the value in X-rays. There is also a small correction for the impurity effect of the thermistors in the calorimeter core. With four thermistors in a core only 20 mm in diameter this correction could be significant, but calculations based on the thermistor composition indicate that the effect is negligible within the uncertainties. A value of 1.000 was used.

The correction factors for the various quantities are given in the Table 3.

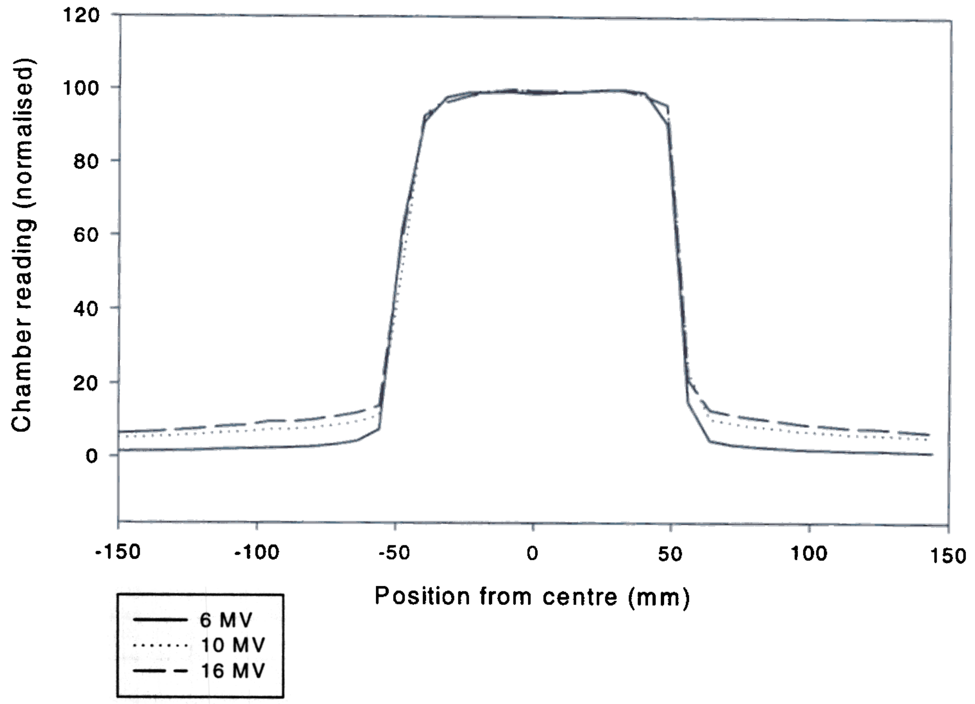

FIG. 8. Beam uniformity measurements in photon beams using linear ion chamber array

Table 3 Summary of correction factors

E_{nom}	Scatter	Depth	Uniformity	Distance	Gap effect	Overall
Photons	*Comparison with NE2611 chamber*					
6 MV	1.0000	1.000	0.9992	1.002	1.0078	1.0090
10 MV	0.9993	1.000	0.9999	1.002	1.0074	1.0086
16 MV	0.9936	1.000	1.0001	1.002	1.0068	1.0025
Electrons	*Comparison with electron calorimeter*					
16 MeV	1.0018	1.000	0.9960	1.000	1.000	0.9978
Electrons	*Comparison with NACP-02 chamber*					
16 MeV	1.0000	1.000	1.0008	1.001	1.000	1.0018

The measurements in 10 MV photons indicated that the scatter contribution due to the body was less than 0.1%. It can be reasonably assumed that the correction at 6 MV would be no larger. As stated above, the body is outside the radiation field and therefore the scatter effect is due to double scattering, which is more likely in higher energy beams. In the 16 MeV electron beam, the scatter correction for the body was not measurable. However, the measurements comparing the 15 × 15 cm and 9 × 9 cm phantoms did show an effect, with a higher reading in the larger phantom, due to increased in-scatter.

4.3.3 Uncertainties

The uncertainties (quoted as standard uncertainties according to UKAS (1995)) in the determination of absorbed dose and calibration of ion chambers in terms of absorbed dose to graphite are given in Table 4.

Table 4 Uncertainties in photon and electron beams

Source	"Random" Standard Uncertainty (%)				"Systematic" Standard Uncertainty (%)
	6 MV	10 MV	16 MV	16 MeV	All qualities
Calorimeter reading	0.20	0.41	0.13	0.20	
Chamber reading	0.08	0.08	0.08	0.10	
Thermistor calibration					0.05
Specific heat capacity					0.08
Gap effect	0.15	0.07	0.07		0.17
Recombination correction					0.10
Beam uniformity	0.05	0.05	0.05	0.05	
Depth correction	0.05	0.05	0.05	0.05	
Scatter correction	0.05	0.05	0.08	0.08	
Thermistor perturbation					0.08
Inverse square correction	0.05	0.05	0.05	0.03	0.10
Charge calibration of electrometer					0.03
Combined standard uncertainty	0.28	0.44	0.20	0.25	0.26
Overall standard uncertainty	0.35	0.50	0.32	0.36	

The uncertainties are split into "random" and "systematic" for the purpose of looking at any energy dependence in the results. The larger uncertainty in the calorimeter reading at 10 MV was due to excessive electrical noise as these measurements were made before the calorimeter was screened properly.

4.3.4 Comparison with primary standards

The results of the comparison of this new calorimeter with the photon and electron primary standard calorimeters are shown in Tables 5 and 6.

Table 5 Results of calorimeter comparison in high energy photons using chamber NE2611 S/N 122

E_{nom} (MV)	Chamber calibration factor (Gy/μC)		Ratio
	Primary standard	Portable calorimeter	Portable/primary std
6	89.84	90.84	1.0112
10	88.18	89.22	1.0119
16	87.10	87.99	1.0102

Table 6 Results of calorimeter comparison in 16 MeV electrons

Device used in comparison	Chamber calibration factor (Gy/μC)		Ratio
	Primary standard	Portable calorimeter	Portable/primary std
NACP S/N N37-01	120.95	126.93	1.049
NACP S/N N30-09	134.79	141.38	1.049
Electron calorimeter	----	----	1.027
Electron calorimeter	----	----	1.066

The first thing to note about the results from the photon measurements is that there is a constant difference between this calorimeter and the photon primary standard. The calibration method of the photon calorimeter is under investigation and it is believed that the dose measured is less than the correct dose by approximately 0.7%. If this is taken into account, then the two calorimeters agree within 0.5% at all energies, which is within the combined measurement uncertainties, and is an encouraging result. Further work is required to extend these measurements to other photon energies including ^{60}Co and to repeat the measurement at 10 MV.

The results from the electron measurements are much less satisfying. The comparisons with the two NACP chambers are consistent but show a difference of almost 5% between the new portable calorimeter and the electron primary standard. This difference is much larger than any possible correction factor and is difficult to explain. The direct comparison with the electron calorimeter sheds some light on the situation and illustrates a problem in electron beam calorimetry. The DC bridge-based temperature sensing system is sensitive to charge storage in the calorimeter core. This is not a significant problem in photon beams since there is charge particle equilibrium and no net charge is stored. However, in an electron beam you can get direct collection of primary electrons and therefore one must ensure that the calorimeter core and surround are properly earthed to prevent any charge build-up. After the first comparison, the electron calorimeter was dismantled and found to have poor earthing connections. It was rebuilt and the calorimeter comparison repeated, yielding a very different answer. The portable calorimeter was left untouched due to lack of time. A more detailed investigation of this problem is required, together with measurements at a number of electron energies.

5. CONCLUSION

Initial testing of the calorimeter has confirmed the suitability of the design. Radiotherapy doserates can be measured with an uncertainty close to that of the present primary standards. The system is portable, opening up the possibility of making direct measurements in user radiation facilities - particularly radiotherapy clinics. Further work is required to improve the temperature control algorithm by modelling of the heat transfer processes in three dimensions. It is hoped to extend this work to model the heat transfer during irradiation and so derive a correction for the heat transfer from core to surround in the calorimeter.

The result of comparing the calorimeter with the present primary standard calorimeter in high energy photon beams is very encouraging, giving agreement within 0.5% of unity at all energies measured. The results in a 16 MeV electron beam are somewhat confusing, showing a discrepancy of approximately 5%. There is no obvious reason for this discrepancy, although a possible cause is charge storage in the calorimeter core due to poor earthing. Further work is required to investigate this problem, as well as carry out a wider range of measurements in both photon and electron beams. Once this work is complete, it is hoped to carry out measurements in UK radiotherapy clinics, as well as other radiation facilities. It should be noted that this calorimeter is not intended to replace the present primary standards, but as a transfer instrument between NPL and other radiation users. This will give a direct determination of absorbed dose where it is required, check the validity of dosimeter calibrations provided at NPL, and allow investigation of issues such as beam quality definition.

6. ACKNOWLEDGEMENTS

The authors would like to acknowledge the financial support of the National Measurement Policy Unit of the UK Department of Trade and Industry.

7. REFERENCES

Boag J W 1950 Ionization measurements at very high intensities. I. Pulsed radiation beams *Brit. J. Radiol.* **23** 601-611

Burns D T, McEwen M R and Williams A J 1994 *An NPL absorbed dose calibration service for electron beam radiotherapy, Proc. Int. Symp. on Measurement Assurance in Dosimetry (IAEA-SM-330/34)* ed S P Flitton (Vienna: IAEA) p61

Burns D T, McEwen M R 1998 Ion recombination corrections for the NACP parallel-plate chamber in a pulsed electron beam *Phys. Med. Biol.* **43** p2033-2045

Cottens E, Janssens A, Eggermont G and Jacobs R 1981 *Absorbed dose calorimetry with a graphite calorimeter, and G-value determinations for the Fricke dosemeter in high energy electron beams, Proc.*

Int. Symp. on Biomedical Dosimetry: Physical Aspects, Instrumentation, Calibration (IAEA-SM-249/32) (Vienna: IAEA) p189

Domen S R and Lamperti P J 1974 *J. Res. Natl. Bur. Stand.* (US) **78** p595

DuSautoy, A R 1996 The UK primary standard calorimeter for photon beam absorbed dose measurement, *Phys. Med. Biol.* **41** p137

McEwen M R, Burns D T and Williams A J 1993 *The use of thermistors in the NPL electron beam calorimeter (NPL Report RSA(EXT)41)* (Teddington: National Physical Laboratory)

McEwen M R, DuSautoy A R and Williams A J 1998 The calibration of therapy level electron beam ionisation chambers in terms of absorbed dose to water *Phys. Med. Biol.* **43** p2503-2519

Richardson M J 1984 *Compendium of thermophysical property measurement methods Vol 1; Survey of measurement techniques, Chapter 17* ed Maglic, Cezairliyan and Peletsky (New York: Plenum Press)

Sanders R P and Thomas C G 1991 *A precision voltage supply for the NPL primary standard electron beam calorimeter (NPL Report RSA(EXT)24)* (Teddington: National Physical Laboratory)

UKAS (United Kingdom Accreditation Service) 1995 *The Expression of Uncertainty and Confidence in Measurement and Calibrations (Report NIS 3003 Edition 8)* (Teddington: UKAS)

Williams A J, Burns D T and McEwen M R 1993 *Measurement of the specific heat capacity of the electron beam graphite calorimeter (NPL Report RSA(EXT)40)* (Teddington: National Physical Laboratory)